Available online at www.sciencedirect.com
SCIENCE DIRECT
Journal of APPLIED MATHEMATICS AND MECHANICS
ELSEVIER
www.elsevier.com/locate/jappmathmech
Journal of Applied Mathematics and Mechanics 69 (2005) 693–704

OPTIMIZATION OF THE SHAPE OF A POROUS SLIDER AS REGARDS LOAD CAPACITY OR STATIC STIFFNESS†

V. I. GRABOVSKII
Moscow
email: vig@ciam.ru

(*Received* 24 *March* 2004)

The problem of an infinite plane porous slider with an isothermal compressible lubricant that is optimum as regards the load capacity or static stiffness of the lubricant layer is solved. The solution is found for the case when there is a prescribed constraint on the lubrication flow rate through the porous insert. The optimum slider shapes found, and also the size and position of the insert, depend on the parameters of the problem that determine the properties of the lubricant and the insert, the supply conditions and the flow rate of the lubricant through the insert.

The feeding of lubricant into the working gap of a gas dynamic bearing improves its operating conditions, including its operation under start-stop conditions, and also increases the load capacity and stiffness of the lubricant layer under working conditions. Among the designs of porous bearings and methods for feeding lubricant into the lubricant layer [1–4], we distinguish bearings having porous inserts with distributed feeding of lubricant [1, 2]. These possess, for example, increased vibration resistance. The operation of bearings with such inserts has been investigated by many researchers who have solved different direct problems. Parametric optimization of the characteristics of a porous radial bearing has been carried out [5]. The optimum shapes of sliders with an impermeable surface and with respect to different parameters have been investigated [6–9].

Below, the problem of determining the optimum shapes of a porous infinite slider that ensure either maximum load capacity or maximum static stiffness of the layer of isothermal compressible lubricant when there is a prescribed constraint on the lubricant flow rate through the porous insert is formulated and solved. Additional lubricant is fed from a reservoir at increased pressure through the insert, where the lubricant flow obeys Darcy's law. Depending on these conditions, the insert may be different length, of equal length or of smaller length than the slider. In the last case it is necessary to determine the optimum size and position of the insert. The introduction of a constraint on the additional flow rate is due to the practical need to reduce the consumption of lubricant and the energy used to supply it, which results in less scope for increasing the load capacity and stiffness.

1. FORMULATION OF THE PROBLEM

Consider a plane slider of length L, infinite in a direction perpendicular to the surface of the drawing in Fig. 1, moving over a plane surface $y = 0$ with a velocity $-U$ in the negative direction of the x axis of a Cartesian system of coordinates x, y, z. The shape of the lower surface of the slider is described by the function $y = h(x)$. In a coordinate system connected to the slider, the surface $y = 0$ moves with a velocity U, while the slider is at rest. The isothermal lubricant with a density ρ proportional to the pressure p has a constant viscosity μ_c. The height of the gap between the slider and the surface satisfies the inequality $h \ll L$ (in Fig. 1 the gap is shown on a magnified scale). The magnitude of the minimum achievable height of the gap h_m, due to the surfaces moving with respect to each other without touching, in specified. Outside the gap (in front of and behind the slider) the pressure of the lubricant is assumed to be constant and equal to p_∞. For a variable height of the gap, the pressure within it $p \neq p_\infty$, and the

†*Prikl. Mat. Mekh.* Vol. 69, No. 5, pp. 775–787, 2005.
0021–8928/$—see front matter.
doi: 10.1016/j.jappmathmech.2005.09.004

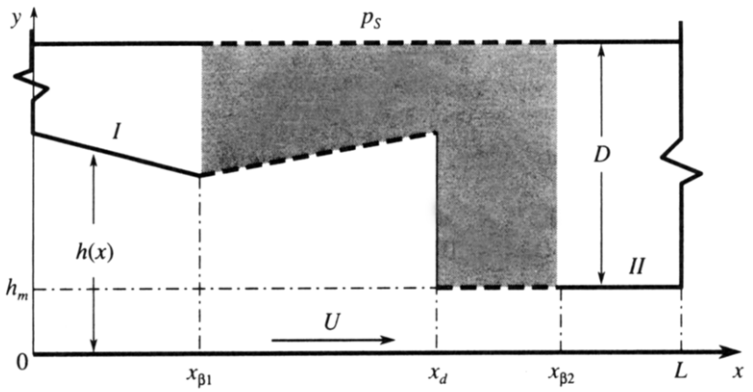

Fig. 1

slider has a load capacity N, which, being equal to the integral of the pressure over the entire surface of the slider, balances out the external load. Along with the load capacity, the static stiffness of the lubricant layer G and the additional lubricant flow rate Q_p through the porous insert are important. Here and below, all the integral characteristics correspond to unit width of the slider in the direction of the z axis.

The slider includes an insert of uniform porosity with thickness $D \gg h_m$ and length $l_p \leq L$ (shown shaded in Fig. 1) and a reservoir with lubricant, the pressure in which $p_s > p_\infty$. Due to the difference in pressures in the reservoir and gap, the lubricant is discharged into the gap. Further, in order to simplify the analysis, we will assume that for a pressure in the porous insert p_p the following inequality holds

$$|\partial p_p/\partial y| \gg |\partial p_p/\partial x|$$

If this inequality is satisfied, the lubricant flows through the porous insert and, on leaving the insert, it flows in the transverse direction y. In addition to this, we will assume that the flow of lubricant in the porous medium obeys Darcy's law [1, 2]. Then the flow density of the lubricant across the insert will be given by the equation

$$j_p(x) = -k_p\mu_c^{-1}\rho\partial p_p/\partial y$$

where k_p is the seepage coefficient.

If the isothermal lubricant is an ideal gas, integration of this equation across the porous layer will give the relation

$$j_p(x) = k_p(2RT\mu_c D)^{-1}(p^2 - p_s^2)$$

where R is the gas constant, T is the absolute temperature, which is assumed to be constant, and $p(x)$ is the pressure in the gap.

The balance equation of the lubricant flow rate stems from the equation of continuity, and for the lubricant in the gap has the form [1, 2]

$$Q' + j_p = 0, \quad Q = \rho\int_0^h u dy$$

The prime denotes a derivative with respect to x, and u is the longitudinal component of the lubricant velocity in the gap. The flow rate Q is expressed in terms of p, p' and h in the well-known way [1, 2] and is given below in dimensionless form. The additional flow rate of lubricant discharged through the porous insert is defined by the integral

$$Q_p = \int_{x_{\beta 1}}^{x_{\beta 2}} j_p dx = Q(x_{\beta 2}) - Q(x_{\beta 1})$$

where $x_{\beta 1}$ and $x_{\beta 2}$ are the longitudinal coordinates of the insert.

We will introduce dimensionless variables with the following scales: L for the coordinates x, h_m for y and h, U for the velocity ad $\gamma\rho_\infty U^2$ for the pressure, where $\gamma = 6\mu_c L(\rho_\infty U h_m^2)^{-1}$. In dimensionless variables, the equation for determining the pressure and the flow rate coefficient q in the gap and the boundary conditions take the form

$$q' + f_\beta(p^2 - P_s^2) = 0, \quad p' = (h - qp^{-1})h^{-3}, \quad p(0) = p(1) = P_\infty, \quad q = 2Q/(\chi\rho_\infty U h_m) \tag{1.1}$$

with the dimensionless complexes (similarity parameters)

$$\beta = 6k_p L^2 h_m^{-3} D^{-1}, \quad P_s = p_s(\gamma\rho_\infty U^2)^{-1}, \quad P_\infty = p_\infty(\gamma\rho_\infty U^2)^{-1}, \quad \chi = \gamma M^2 = P_\infty^{-1} \tag{1.2}$$

In view of the inequality $l_p \leq L$, a piecewise-constant function f_β is introduced, defined as

$$f_\beta = \beta \text{ when } x_{\beta 1} \leq x \leq x_{\beta 2} \text{ and } f_\beta = 0 \text{ when } x < x_{\beta 1}, \quad x_{\beta 2} < x \tag{1.3}$$

where $x_{\beta 1}$ and $x_{\beta 2}$ define the size and position of the insert (Fig. 1).

The solution of problem (1.1) depends on the similarity parameters β, P_s and χ, which characterize the porosity of the insert, the supply pressure and the compressibility of the lubricant. Like the flow rate coefficient q introduced earlier, we will define the coefficients of the load capacity C_N, stiffness C_G and additional flow rate by the equalities

$$C_N = \frac{N}{\gamma L\rho_\infty U^2} = \int_0^1 p\,dx - P_\infty, \quad C_G = \frac{G}{\gamma L\rho_\infty U^2}, \quad q_p = 2Q_p/(\chi\rho_\infty U h_m) \tag{1.4}$$

The static stiffness G of the lubricant layer and its coefficient C_G will be determined in the following way [4]. Let the slider perform a small quasi-steady displacement along the y axis by an amount $\varepsilon \ll 1$. Then the height of the gap, the pressure and the flow rate within it can be represented in the form

$$h = h_0 - \varepsilon, \quad p = p_0 + \varepsilon p_1, \quad q = q_0 + \varepsilon q_1 \tag{1.5}$$

The functions $h_0(x)$, $p_0(x)$ and $q_0(x)$ satisfy the equations and boundary conditions (1.1) with a zero subscript on all the variables.

Introducing the stiffness by the equation [4] $G = dN/d\varepsilon$, using relations (1.4) and (1.5) we obtain

$$C_G = \int_0^1 p_1\,dx \tag{1.6}$$

The differential equation and the boundary conditions for a perturbation of the pressure p_1, obtained from relations (1.1) and (1.5), take the form

$$p_1' = (2p_0 + q_0 p_1 p_0^{-1} - q_1 - 3q_0 h_0^{-1})p_0^{-1}h_0^{-3}, \quad p_1(0) = p_1(1) = 0 \tag{1.7}$$

The quantity q_1 is defined by the equation

$$q_1' + 2f_\beta p_0 p_1 = 0 \tag{1.8}$$

Thus, the load capacity is determined from the unperturbed pressure p_0, and the static stiffness is determined from its perturbation p_1.

The model used corresponds to subsonic flows. An incompressible lubricant corresponds to $M^2 \ll 1$, $\chi \ll 1$, and a greatly compressible lubricant corresponds to $M^2 < 1$, $\chi \gg 1$. The case $\beta = 0$ corresponds to a slider without a porous insert.

We will estimate the similarity parameters for real cases. If

$$U = 10^2 \text{ m/s}, \quad T = 300 \text{ K}, \quad L = 0.1 \text{ m}, \quad h_m = 2 \times 10^{-5} \text{ m}, \quad \mu_c = 1.75 \times 10^{-5} \text{ Pa s},$$

$$p_\infty = 0.98 \times 10^5 \text{ Pa}, \quad \rho_\infty = 1.3 \times 10^3 \text{ g m}^{-3}, \quad D = 5 \times 10^{-3} \text{ m}, \quad k_p = 10^{-14} \text{ m}^2$$

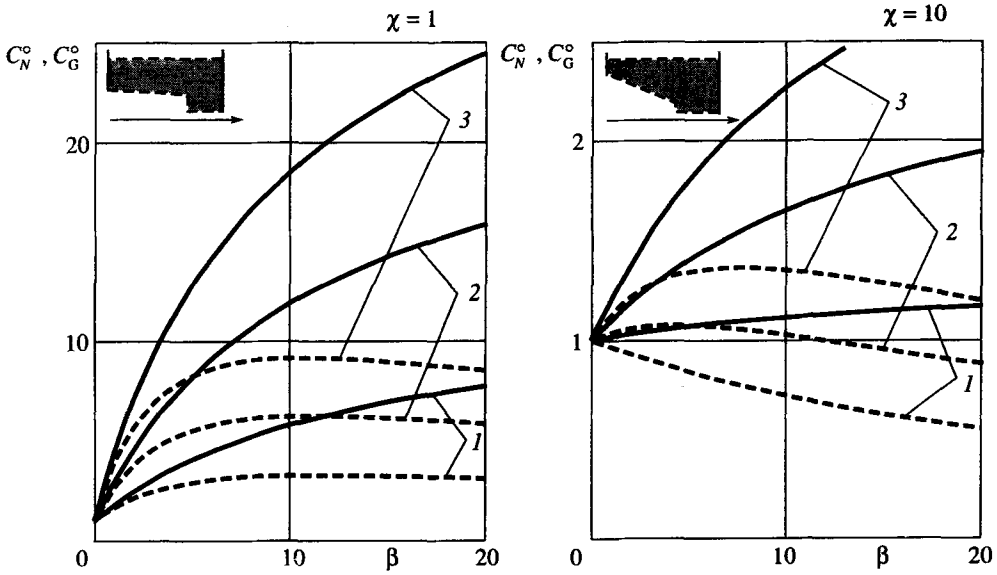

Fig. 2

then

$$\gamma \approx 2 \times 10^2, \quad \chi \approx 26, \quad M^2 \approx 0.13, \quad \beta \approx 15$$

We will give the results of the solution of direct problems for porous sliders with a prescribed Rayleigh gap (for which the greatest load capacity when $\beta = 0$ is obtained [6, 7]). The solution is found by numerical integration of Eqs (1.1), (1.7) and (1.8) for a specified function $h_0(x)$ and $x_{\beta 1} = 0, x_{\beta 2} = 1$ (the entire slider is porous $-l_p = L$). Figure 2 shows graphs of $C_N^\circ = C_N(\beta)/C_N(0)$ (the continuous curves) and $C_G^\circ = C_G(\beta)/C_G(0)$ (the dashed curves) for $\chi = 1$ ($C_N(0) = 0.0343$, $C_G(0) = 0.0683$) and 10 ($C_N(0) = 0.0304$, $C_G(0) = 0.0507$). The corresponding sliders are also shown. Curves 1, 2 and 3 correspond to $P_s/P_\infty = 1.5, 2, 2.5$. An increase in P_s is always accompanied by an increase in the load capacity and the stiffness. The function $C_N^\circ(\beta)$ is monotonic, and $C_G^\circ(\beta)$ has a maximum, the magnitude and coordinate β^m of which depend on the values of P_s and χ. In practice, case of a simultaneous increase in the parameters C_N and C_G are of interest. When $\chi = 10$ the region $[0, \beta^m]$ is considerably greater than when $\chi = 10$. Its extent also increases when the parameter P_s increases.

Note that an increase in the load capacity and stiffness is accompanied by an undesirable increase in the additional lubricant flow rate through the porous insert. For fixed values of β and P_s and with $l_p = L$, the coefficient q_p is a maximum. When the parameters β and P_s increase, this quantity $q_{p,\max}$ increases.

2. THE OPTIMUM SLIDERS

The sliders investigated above are not optimum in terms of load capacity when $\beta > 0$ and are not optimum in terms of stiffness whatever the value of β. We will consider the problem of determining the shape of the slider and also the size and position of the porous insert that, for specified β, P_s and χ, ensure either maximum load capacity or maximum static stiffness, when there is a constraint on the magnitude of the additional flow rate.

Sliders of optimum load capacity. It is required to find the function $h_0(x)$ and the coordinates $x_{\beta 1}$ and $x_{\beta 2}$ that ensure a maximum of the functional C_N taking into account the differential relations (1.1) with subscript, the constraints on the height of the gap $1 \le h_0(x)$ and the additional flow rate $q_p \le q_{p,\max}$.

To solve the problem, we will set up the Lagrange functional

$$J_N = C_N + \int_0^1 F_N dx + \alpha q_p; \quad F_N = \lambda(p_0 h_0 - q_0 - p_0 h_0^3 p_0') + \mu(q_0' + f_\beta(p_0^2 - P_s^2)) \qquad (2.1)$$

in which $\lambda(x)$ and $\mu(x)$ are variable and α is a constant Lagrange multipliers. When $\alpha = 0$ the problem changes into one without a constraint on the magnitude of q_p, and we obtain $l_p = L$ and $q = q_{p,\max}$.

To obtain the necessary conditions of optimality, the function J_N is varied according to well-known rules [8]. If the gap is optimum, i.e. a maximum of C_N is attained, the variations $\Delta C_N = \Delta J_N \leq 0$ for any variations δh_0 satisfying the constraint on the height $h_0(x)$. Variation is carried out taking into account the continuity of p_0 and q_0 in the sections $x = x_d$ of possible discontinuities of the function h_0. Their presence is a characteristic feature of optimum sliders. In these sections, the Lagrange multipliers may also have a discontinuity. Other characteristics sections are $x = x_{\beta 1}$ and $x = x_{\beta 2}$, where the function f_β and one of the Lagrange multipliers undergoes a discontinuity. The position of these discontinuities is unknown and is determined when solving the problem.

After the necessary calculations, for the variation $\Delta C_N = \Delta J_N$ we obtain

$$\Delta C_N = \sum_{d,\beta 1,\beta 2} \{-[\lambda h_0^3]p_0\Delta p_0 + [\mu]\Delta q_0 + [\lambda p_0 h_0^3 p_0' - \mu q_0']\Delta x\} + \alpha(\Delta q_{0,\beta 2} - \Delta q_{0,\beta 1}) +$$

$$+ (\mu\Delta q_0)_{x=1} - (\mu\Delta q_0)_{x=0} + \int_0^1 \{P\delta p_0 + B\delta h_0 - (\lambda + \mu')\delta q_0\}dx \tag{2.2}$$

$$P = p_0(\lambda h_0^3)' + \lambda h_0 + 1 + 2\mu f_\beta p_0, \quad B = \lambda(3q_0 h_0^{-1} - 2p_0); \quad [w] = w_- - w_+$$

Summation is carried out over all the sections indicated above, where the function h_0 or the function f_β undergoes a discontinuity. The square brackets denote a discontinuity of the parameter in the corresponding section, while the minus and plus subscripts are ascribed to this parameter before and after the discontinuity respectively. In expression (2.2), Δx, Δp_0 and Δq_0 are increments of the x coordinate, the pressure p_0 and the flow rate q_0 in the sections $x = 0, x = 1, x = x_d, x = x_{\beta 1}$ and $x = x_{\beta 2}$.

According to expression (2.2), the following problem is formulated for the Lagrange multipliers λ and μ for any (including non-optimum) gaps that may be formed by the piecewise-continuous function $h_0(x)$.

$$(\lambda h_0^3)' + (\lambda h_0 + 1)p_0^{-1} + 2\mu f_\beta = 0, \quad [\lambda h_0^3]_d = 0, \quad [\lambda]_{\beta 1} = 0, \quad [\lambda]_{\beta 2} = 0 \tag{2.3}$$

$$\mu' + \lambda = 0, \quad \mu(0) = \mu(1) = 0, \quad [\mu]_d = 0, \quad [\mu]_{\beta 1} = \alpha, \quad [\mu]_{\beta 2} = -\alpha \tag{2.4}$$

One of the boundary conditions in (2.4) for the multiplier μ is satisfied by the choice of quantity $\lambda(0)$. The conditions at the discontinuities in relations (2.3) and (2.4) indicate that both functions $\mu(x)$ and $\lambda(x)$ may be discontinuous. For multipliers λ and μ satisfying equations and conditions (2.3) and (2.4), expression (2.2) takes the form

$$\Delta C_N = \sum_{d,\beta 1,\beta 2} \{[\lambda p_0 h_0^3 p_0' - \mu q_0']\Delta x\} + \int_0^1 B\delta h_0 dx \tag{2.5}$$

in which all the variations and increments can be assumed to be independent.

Since the increments Δx may be arbitrary, it follows that, with the optimum position of the given discontinuities of the functions, the coefficients of Δx should vanish. Hence, taking into account the conditions at discontinuities (2.3) and (2.4), the differential equations (1.1) (for functions with zero subscripts) and the discontinuity of p_0 and q_0, we obtain the relations

$$\lambda_{d-}\{p_0 h_{0-} - q_0 - h_{0-}^3 h_{0+}^{-3}(p_0 h_{0+} - q_0)\} = 0, \quad \mu_{\beta 1+} = 0, \quad \mu_{\beta 2-} = 0 \tag{2.6}$$

which define the sections x_d, $x_{\beta 1}$ and $x_{\beta 2}$ in the optimum slider. From relations (2.6) and (2.3), (2.4) it follows that

$$\lambda_{d-} = \lambda_{d+} = 0, \quad \mu_{\beta 1-} = \alpha, \quad \mu_{\beta 2+} = \alpha$$

Thus, the multiplier λ is continuous everywhere and passes through zero in the section $x = x_d$, while the multiplier μ undergoes a discontinuity in the sections $x_{\beta 1}$ and $x_{\beta 2}$.

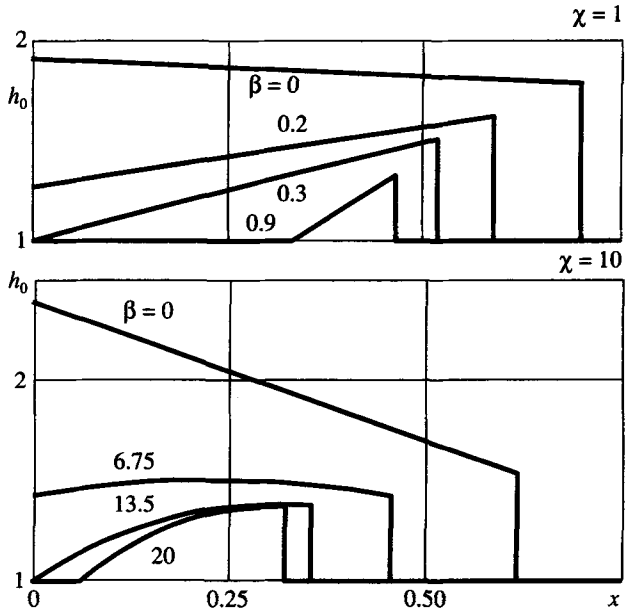

Fig. 3

In part of the slider where $h_0 > 1$, the variations δh_0 are arbitrary, and the corresponding condition of optimality takes the form

$$\lambda(3q_0h_0^{-1} - 2p_0) = 0 \tag{2.7}$$

Equation (2.7), corresponding to the segment of the two-sided extremum (1), enables us to determine the height of the gap on it

$$h_0 = 3q_0p_0^{-1}/2 \tag{2.8}$$

In the part of the slider where $h_0 = 1$ (the segment of the boundary extremum (II)), the permissible variations $\delta h_0 > 0$. Therefore, here the condition for a maximum of C_N is formulated, in accordance with relation (2.5), in the form of the inequality

$$\lambda(3q_0h_0^{-1} - 2p_0) < 0 \tag{2.9}$$

From an analysis of the equations of lubrication and the conditions of optimality obtained, the structure of the optimum solution follows. The function $h_0(x)$ contains two segments of optimality (I and II) which join in a discontinuous way in the section $x = x_d$. The ends of the porous insert are always found in different segments.

Thus, the problem reduces to a numerical calculation of the multipliers λ and μ from differential equations (2.3) and (2.4) and the functions p_0, q_0 and h_0 from Eqs (1.1) and (2.8) on each of the segments indicated. Then the maximum coefficient C_N and the functions $p_1(x)$ and $q_1(x)$ accompanying it (by integration of Eqs (1.7) and (1.8)) and the non-optimum coefficient C_G are calculated.

The results of calculations for $P_s/P_\infty = 2$, *different values of* β *and* χ *and* $\alpha = 0$. This case corresponds to the absence of a flow rate constraint. Then the entire slider is porous ($x_{\beta 1} = 0$, $x_{\beta 2} = 1$) and $q_p = q_{p,\max}$. Figure 3 shows the optimum shapes of such sliders for $\chi = 1$ and $\chi = 10$. The curves $\beta = 0$ correspond to the optimum Rayleigh sliders with impermeable surfaces. A change in the shape of the slider occurs as β increases with a reduction in gap height. Here, two factors counteract each other – motion of the slider (the dynamic effect) and feeding of the lubricant (the static effect). The first tends to increase the front part of the gap, and the second tends to reduce it. As β increases, the second factor begins to predominate, leading to a reduction in the gap height in section $x = 0$ and to the formation of a hollow in the slider. The function $h_0(x)$ is always discontinuous in the section $x = x_d$. For large values of β, the lubricant may leak out of the gap through both sections $x = 0$ and $x = 1$.

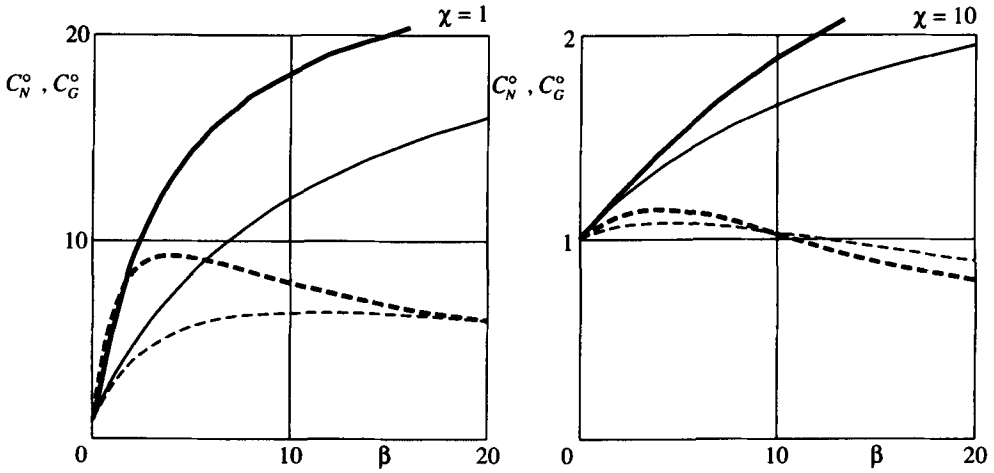

Fig. 4

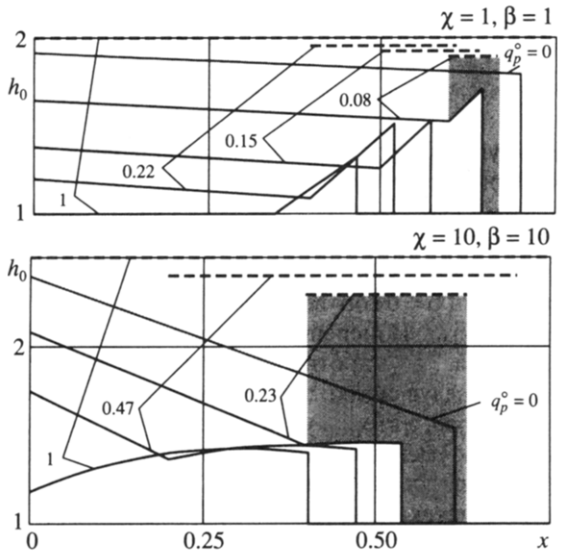

Fig. 5

Figure 4 shows the change, as the parameter β increases, in the optimum coefficient C_N° (the thick continuous curves) and in the non-optimum coefficient C_G° (the thick dashed curves), determined in the same way as in Fig. 2, from which we have taken relations (the thin curves) corresponding to Rayleigh sliders that are non-optimum when $\beta > 0$ with the same parameters. The gain in load capacity is considerable, for example, for $\beta = 10$, it is about 50% when $\chi = 1$ and 15% when $\chi = 10$. For low values of β there is a simultaneous increase in C_G°, i.e. these shapes, optimum in terms of load capacity, also possess increased stiffness. For large values of β, this is not so.

Results of calculations for $P_s/P_\infty = 2$, *different values of* β *and* χ *and* $\alpha \neq 0$. Different values of α correspond to different values of additional flow rate of lubricant through the porous insert $q_p < q_{p,\max}$. The length of the insert becomes smaller than that of the slider $(x_{\beta 2} - x_{\beta 1}) < 1$. The coordinates $x_{\beta 1}, x_{\beta 2}$ and the flow rate q_p coefficient are found from the solution of the problem. Figure 5 shows the shapes of the optimum sliders for $\chi = 1, \beta = 1$ ($q_{p,\max} = 2.587$) and $\chi = 10, \beta = 10$ ($q_{p,\max} = 0.146$) for different relative coefficients $q_p^\circ = q_p/q_{p.\max}$. The rectilinear horizontal dashed segments show the positions of the porous inserts, defined by the coordinates $x_{\beta 1}$ and $x_{\beta 2}$. As an example, the shaded area denotes the corresponding inserts for one of the versions of each values of χ. In a similar way it is possible to show inserts for other values of q_p°.

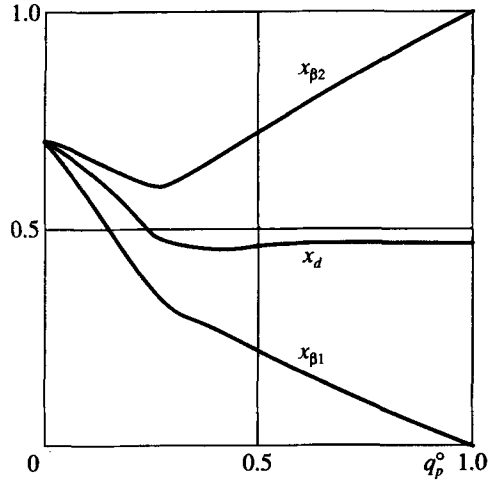

Fig. 6

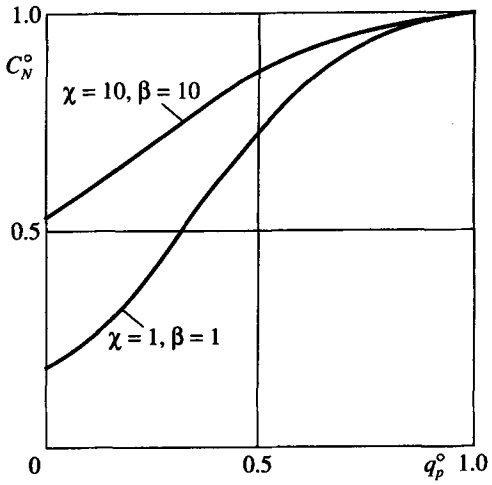

Fig. 7

The lines $q_p^\circ = 0$ correspond, as in Fig. 3, to impermeable Rayleigh sliders. It is significant that the optimum position of the insert is in the middle part of the slider, close to section x_d, and here it is always the case that $x_{\beta 1} < x_d < x_{\beta 2}$. This is illustrated in Fig. 6, where the dependence of the coordinates $x_{\beta 1}$, $x_{\beta 2}$, x_d on the parameter q_p° in accordance with Fig. 5 for the first case when $\chi = 1$ is shown.

It can be seen that a reduction in q_p is accompanied by a reduction in load capacity. In Fig. 7 the level of this reduction is illustrated by the relations $C_N^\circ(q_p^\circ) = C_N(q_p)/C_N(q_{p,\max})$ for the optimum sliders from Fig. 5 ($\chi = 1 - C_{N,\max} = 0.186$, $\chi = 10 - C_{N,\max} = 0.058$).

Optimum sliders in terms of the static stiffness of the lubricant layer. It is required to find the maximum functional (1.6) using relations (1.1), (1.7) and (1.8), under conditions of the gap height constraint indicated earlier and a possible constraint on the quantity q_p. The corresponding Lagrange functional has the form

$$J_G = C_G + \int_0^1 \{F_N + \lambda_1(q_0 p_1 p_0^{-1} - 3q_0 h_0^{-1} + 2p_0 - q_1 - h_0^3 p_0 p_1') + \mu_1(q_1' + 2f_\beta p_0 p_1)\}dx + \alpha q_p$$

with additional, Lagrange multipliers $\lambda_1(x)$ and $\mu_1(x)$ compared with the functional J_N. Note that the functional J_G contains the function F_N from integral (2.1). Analysis of this functional for a maximum is carried out in the same way as above.

Now the problem for the Lagrange multipliers is formulated as follows:

$$\begin{aligned} &(\lambda h_0^3)' + \lambda h_0 p_0^{-1} + \lambda_1 p_0^{-2}(q_1 + q_0(3p_0 - 2p_1 h_0)p_0^{-1}h_0^{-1}) + 2f_\beta(\mu + \mu_1 p_1 p_0^{-1}) = 0 \\ &[\lambda h_0^3]_d = 0, \quad [\lambda]_{\beta 1} = 0, \quad [\lambda]_{\beta 2} = 0 \end{aligned} \tag{2.10}$$

$$(\lambda_1 h_0^3)' + (\lambda_1 h_0 + 1)p_0^{-1} + 2f_\beta \mu_1 = 0; \quad [\lambda_1 h_0^3]_d = 0, \quad [\lambda_1]_{\beta 1} = 0, \quad [\lambda_1]_{\beta 2} = 0 \tag{2.11}$$

$$\mu' + \lambda + \lambda_1(3h_0^{-1} - p_1 p_0^{-1}) = 0; \quad \mu(0) = \mu(1) = 0, \quad [\mu]_d = 0, \quad [\mu]_{\beta 1} = \alpha, \quad [\mu]_{\beta 2} = -\alpha \tag{2.12}$$

$$\begin{aligned} &\mu_1' + \lambda_1 = 0; \quad \mu_1(0) = \mu_1(1) = 0, \quad [\mu_1]_d = 0, \quad [\mu_1]_{\beta 1} = 0, \quad [\mu_1]_{\beta 2} = 0 \\ &[w] = w_- - w_+ \end{aligned} \tag{2.13}$$

The square brackets mean the same as in expressions (2.2)–(2.4). The values of $\lambda(0)$ and $\lambda_1(0)$, necessary for the integration of Eqs (2.10) and (2.11), are unknown in advance and are selected by satisfying the second conditions from relations (2.12) and (2.13). The conditions in sections $x_{\beta 1}$, x_d and $x_{\beta 2}$, determining their optimum position, have the form

$$\lambda_{d-}\{p_0h_{0-} - q_0 - h_{0-}^3 h_{0+}^{-3}(p_0h_{0+} - q_0)\}_d +$$

$$+ \lambda_{1d-}\{q_0p_1p_0^{-1} - 3q_0h_{0-}^{-1} + 2p_0 - q_1 - h_{0-}^3 h_{0+}^{-3}(q_0p_1p_0^{-1} - 3p_0h_{0+}^{-1} + 2p_0 - q_1)\}_d = 0$$

$$\mu_{\beta 1+} = 0, \quad \mu_{\beta 2-} = 0$$

Analysis of the variation of functional J_G and the optimality conditions obtained indicate that the solution of the problem has the same features as for the case of maximum load capacity. To be precise, there are two segments of optimality (the two-sided extremum (I) and the boundary extremum (II)) joining with a discontinuity of the function $h_0(x)$ or without a discontinuity, depending on the values of the parameters of the problem. On the segment of the two-sided extremum, the condition of optimality, determining the function $h_0(x)$, reduces to the question

$$\lambda(3q_0 - 2p_0h_0)h_0 + 3\lambda_1\{q_1h_0 - 2p_0h_0 + q_0(4 - h_0p_1p_0^{-1})\} = 0 \tag{2.14}$$

On the segment of the boundary extremum ($h_0 = 1$) the condition of optimality corresponds to the requirement that the left-hand side of Eq. (2.14) should be negative.

In the section $x = x_d$ of the discontinuity of the height of the optimum gap, the multipliers μ and μ_1 are continuous, while the multipliers λ and λ_1 can become discontinuous. At the ends of the porous insert, the coordinates of which $x_{\beta 1}$ and $x_{\beta 2}$ are determined in the course of the solution, the multiplier μ becomes discontinuous with continuous multipliers μ_1, λ and λ_1. The above equations and relations enable us to find the shapes of the sliders with the greatest static stiffness for different values of the parameters. The problem reduces to a numerical calculation of λ, λ_1, μ and μ_1 from the differential equations and conditions (2.10)–(2.13), p_0, q_0 and h_0 from Eqs (1.1) and (2.14), and also p_1 and q_1 from Eqs (1.7) and (1.8) on each of the segments indicated.

Results of calculations for $P_s/P_\infty = 2$, *different values of* β *and* χ *and* $\alpha = 0$. This case corresponds to the case when there is no constraint on the flow rate q_p. The entire slider is porous ($x_{\beta 1} = 0, x_{\beta 2} = 1$) and $q_p = q_{p,\max}$. The special case $\beta = 0$ for an impermeable slider with an incompressible lubricant was investigated earlier [9]. For a compressible lubricant, Fig. 8 shows the optimum sliders when $\chi = 1$ and $\chi = 10$. The dot-and-dash curves give the corresponding Rayleigh sliders from Fig. 3; the remaining curves correspond to stiffness-optimum sliders for different β. The $\beta = 0$ curve corresponds to an impermeable slider. At low compressibility ($\chi = 1$) the presence of projections, when there is a discontinuity of the function h_0, is characteristic. When the parameter β increases, the height of the gap $h_0(x)$ becomes continuous and decreases.

Figure 9 shows the change in the optimum coefficient C_N° (the dashed curves) and the accompanying non-optimum coefficient C_N (the continuous curves) as the parameter β increases. The corresponding relations for non-optimum sliders (for the Rayleigh shape from Fig. 2) with the same parameters are represented by the thin curves. The gain in stiffness turns out to be considerable. For example, for $\beta = 5$ it is about 65% when $\chi = 1$ and 9% when $\chi = 10$. For such sliders, a gain in load capacity is also always obtained.

Results of calculations for $P_s/P_\infty = 2$, $\chi = 1$, $\beta = 0.2$ *and* $\alpha \neq 0$. The results relate to different values of the prescribed lubricant flow rate through the porous insert $q_p < q_{p,\max}$. Unlike the case when $\alpha = 0$, the length of the insert becomes smaller that the length of the slider. Figure 10 shows the shapes of the optimum sliders for different values of the relative coefficients $q_p^\circ = q_p/q_{p,\max}$ ($q_{p,\max} = 0.578$). The rectilinear dashed segments show the positions of the porous inserts defined by the coordinates $x_{\beta 1}$ and $x_{\beta 2}$. As in Fig. 5, one of the inserts ($q_p^\circ = 0.03$) has been shaded.

The q_p° curve corresponds, as in Fig. 8 with $\beta = 0$, to an impermeable slider. It is significant that the optimum position of the insert, as in sliders that are optimum in terms of load capacity, is in the middle part of the slider. The dependences of coordinates x_d, $x_{\beta 1}$ and $x_{\beta 2}$ on parameter q_p° behave qualitatively as in Fig. 6.

A reduction in q_p is accompanied by a reduction in stiffness. In Fig. 11 the level of this reduction is illustrated by the dependences of C_G° (dashed curves) and C_N° (continuous curves) on q_p° for optimum sliders from Fig. 10 ($C_{G,\max} = 0.136$, $C_{N,\max} = 0.053$).

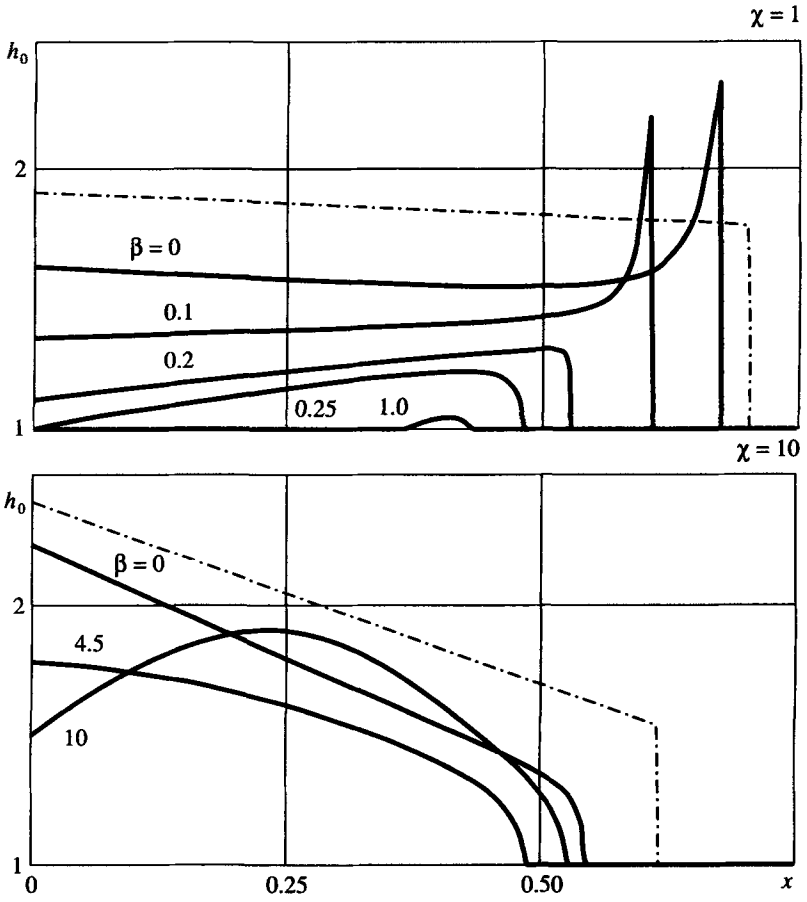
χ = 1
h_0
2
β = 0
0.1
0.2
0.25
1.0
1
χ = 10
h_0
β = 0
2
4.5
10
1
0
0.25
0.50
x

Fig. 8

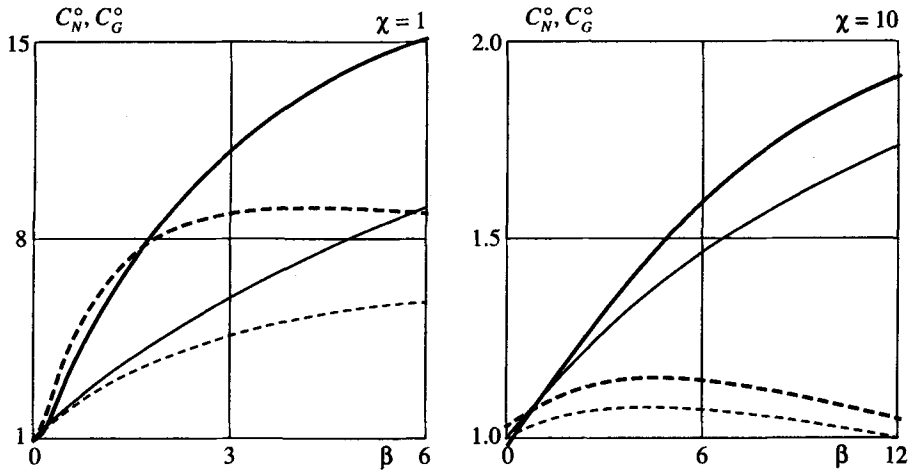
C_N°, C_G°
χ = 1
15
8
1
0
3
β 6
C_N°, C_G°
χ = 10
2.0
1.5
1.0
0
6
β 12

Fig. 9

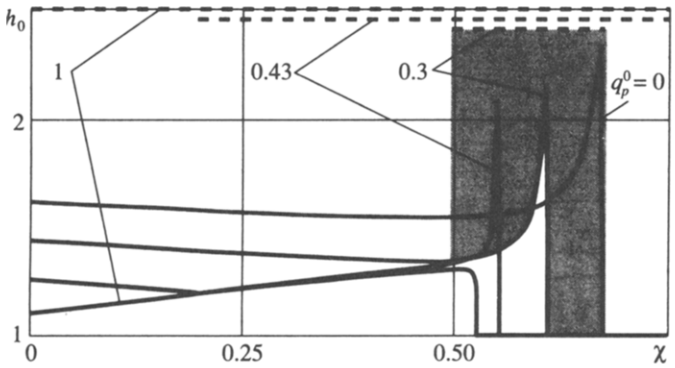

Fig. 10

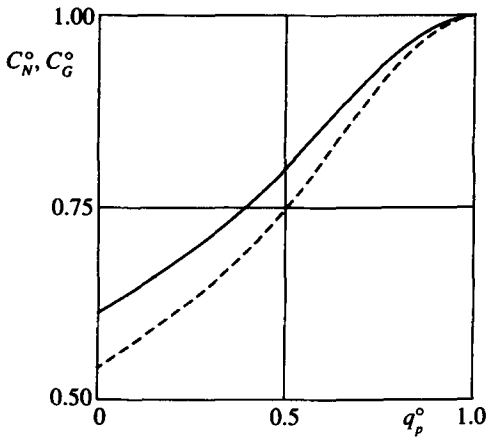

Fig. 11

3. CONCLUSIONS

The problem of determining the optimum shapes of an infinite plane porous slider with an isothermal compressible lubricant that ensure either the greatest load capacity or the greatest static stiffness of the lubricant layer, given a constraint on the lubricant flow rate through the porous surface, has been formulated and solved. It has been shown that, depending on the parameters of the problem – the compressibility of the lubricant χ, the porosity β and the supply pressure P_s – the height of the gap of the optimum slider can be both a continuous and a discontinuous function of the longitudinal coordinate. As the parameters β and P_s increase, the load capacity increases while the stiffness has a maximum. In a certain range of variation in parameter β, both characteristics are increasing.

The optimum slider shapes obtained can yield a gain in load capacity and stiffness, compared, for example, with an impermeable Rayleigh slider, of up to 100% at $\chi = 1$. When the compressibility increases, the gains decrease appreciably. There are ranges of the governing parameters where slider shapes are obtained both with a high load capacity and high stiffness.

A constraint on the magnitude of the lubricant flow rate through the porous insert is achieved by reducing the parameters β and P_s, and also the longitudinal dimensions of the porous insert, which is accompanied by losses in load capacity and static stiffness. It has been shown that the optimum insert position is in the middle part of the slider.

I wish to thank A. N. Kraiko for helpful suggestions.

This research was supported by the Russian Foundation for Basic Research (02-01-00422) and the "State Support for Leading Scientific Schools" Programme (NSh-2124.2003.1).

REFERENCES

1. CONSTANTINESCU, V. N., *Lubricatie cu Gaze*. Editura Acad. Rep. Popul. Romine, Bucharest, 1963.
2. SHEINBERG, S. A., ZHED', V. P. and SHISHEYEV, M. D., *Gas Slider Bearings*. Mashinostroyeniye, Moscow, 1969.
3. PINEGIN, S. V., TABACHNIKOV, Yu. B. and SIPENKOV, I. Ye., Static and dynamic characteristics of gas static bearings. Nauka, Moscow, 1982.
4. PESHTI, Yu. V., *Gas Lubricant*. Izd. MGTU, Moscow, 1993.
5. MARINKOVIC, A., ROSOC, B. and JANKOVIC, M., Optimum design for porous metal bearing. *Int. J. Appl. Mech. and Eng.*, 2002, **7**, 3, 875–885.
6. MADAY, C. J., The one-dimensional optimum hydrodynamic gas slider bearing. *Trans. ASME. Ser. F. J. Lubr. Technol.*, 1968, **90**, 1, 281–284.
7. GRABOVSKII, V. I., Optimum design of a slider, ensuring it minimum drag. *Izv. Ros. Akad. Nauk. MZhG*, 1999, 2, pp. 14–25.
8. KRAIKO, A. N., The isoperimetric problem of design the optimum gap of an infinite plane slider. *Prikl. Mat. Mekh.*, 1998, **62**, 222–233.
9. GRABOVSKII, V. I., The determination of the gap of a plane slider which gives maximum stiffness. *Izv. Ros. Akad. Nauk, MZhG*, 2003, 6, 16–23.

Translated by P.S.G.